

## Supporting Information

### Interfacial Electric Field of BiVO<sub>4</sub>/WO<sub>3</sub> Photoanode Induced S-scheme Charge Transfer for Enhanced Photoelectrochemical Performance

Jian Zuo <sup>a</sup>, Huili Guo <sup>a</sup>, Shu Chen <sup>a\*</sup>, Yong Pei <sup>b, c\*</sup>, Canjun Liu <sup>a, b</sup>

<sup>a</sup> Key Laboratory of Theoretical Organic Chemistry and Function Molecule of Ministry of Education, School of Chemistry and Chemical Engineering, Hunan University of Science and Technology, Xiangtan 411201, Hunan, China

<sup>b</sup> School of Chemistry, Xiangtan University, Xiangtan 411105, China

<sup>c</sup> State Key Laboratory of Complex Nonferrous Metal Resources Clean Utilization, Kunming University of Science and Technology, Kunming 650093, China

\*Corresponding author. Tel.: +86 731 5829 0045; fax: +86 731 5829 0045.

E-mail addresses: chenshu@hnust.edu.cn; ypnku78@gmail.com;

#### Related calculation process

The band gap ( $E_g$ ) of the samples can be obtained by converting the absorption curve into a Tauc plot according to the equation as follows:

$$(\alpha h\nu) = A^0(h\nu - E_g)^n \quad \text{Equation S1}$$

where  $\alpha$ ,  $h$ ,  $\nu$ , and  $A^0$  are the absorbance of the film, Planck's constant, frequency of light, and material-related constants, respectively. For indirect band gap semiconductors,  $n=2$ . But in case of direct band gap semiconductors,  $n=1/2$ . As shown

in Fig. S2b, the  $E_g$  is 2.47 eV for BiVO<sub>4</sub> and 2.48 eV for BiVO<sub>4</sub>/WO<sub>3</sub>. The similar band gaps of them correspond to their light absorption ranges.

The flat-band potential ( $E_{fb}$ ), carrier concentration ( $N_d$ ) and depletion widths ( $W_d$ ) can be calculated by the following equations:

$$\frac{1}{C^2} = \frac{1}{q\epsilon\epsilon_0 N_d} \left( E - E_{fb} - \frac{kT}{q} \right) \quad \text{Equation S2}$$

$$W_d = \left[ \frac{2\epsilon\epsilon_0 \left( E - E_{fb} - \frac{kT}{q} \right)}{qN_d} \right]^{1/2} \quad \text{Equation S3}$$

Where  $C$ ,  $q$ ,  $\epsilon_0$ ,  $k$  and  $V_E$  are the capacitance of space charge region, the electronic charge, the vacuum permittivity, the Boltzmann constant and the applied potential, respectively.  $kT/q$  can be ignored at room temperature.

The charge transfer efficiency ( $\eta_{trans}$ ) and separation efficiency ( $\eta_{sep}$ ) were calculated for BiVO<sub>4</sub> and BiVO<sub>4</sub>/WO<sub>3</sub> using the following equations:

$$\eta_{trans} = J/J_{sulfite} \quad \text{Equation S4}$$

$$\eta_{sep} = J_{sulfite}/J_{abs} \quad \text{Equation S5}$$

where  $J$  and  $J_{sulfite}$  are the photocurrent of water oxidation without any scavenger and the oxidation current of Na<sub>2</sub>SO<sub>3</sub>.  $J_{abs}$  is the rate of photon absorption expressed as a current density.

The transient photocurrent data were fitted using the following equations:

$$D = \exp(-t/\tau_t) \quad \text{Equation S6}$$

$$D = (I_t - I_f)/(I_i - I_f) \quad \text{Equation S7}$$

where  $I_t$ ,  $I_f$ , and  $I_i$  are the time-dependent, the steady-state and the initial

photocurrents, respectively. The transient time constant ( $\tau_t$ ) is defined as the time when  $\ln D = -1$ , which reflects the recombination degree of photogenerated electrons and holes and measures the lifetime of photogenerated electrons.

The work function ( $W_f$ ), and valence band potential ( $E_{VB}$ ) and conductive band potential ( $E_{CB}$ ) of  $\text{BiVO}_4$  and  $\text{WO}_3$  versus vacuum energy level (vac) and normal hydrogen electrode (NHE) can be calculated using the following equations<sup>1,2</sup>:

$$W_f = h\nu - E_{cutoff} \quad \text{Equation S8}$$

$$E_{VB} = W_f + E_{edge} \quad \text{Equation S9}$$

$$E_{CB} = E_{VB} - E_g \quad \text{Equation S10}$$

$$E_{NHE} = -E_{vac} - 4.5 \quad \text{Equation S11}$$

where  $h\nu$  (21.22 eV) is the excitation energy;  $E_{cutoff}$  is the secondary electron cut-off edges;  $E_{edge}$  is the Fermi edges;  $E_g$  is the band gap of photoanode, using 2.4 eV<sup>3</sup> and 2.8 eV<sup>4</sup> for  $\text{BiVO}_4$  and  $\text{WO}_3$ , respectively.

### **DFT calculations**

The work function and electron density difference calculations were conducted by using CASTEP module of Materials Studio (MS). The GGA with the revised PBE functional was used to describe the exchange-correlation potential. Ultrasoft pseudopotentials was chosen to cope with ion cores. SCF tolerance is  $5.0 \times 10^{-7}$  eV/atom for energy calculation and  $5.0 \times 10^{-6}$  eV/atom for geometry optimization. During geometry optimization, the convergence force was below 0.01 eV/Å on each atom.

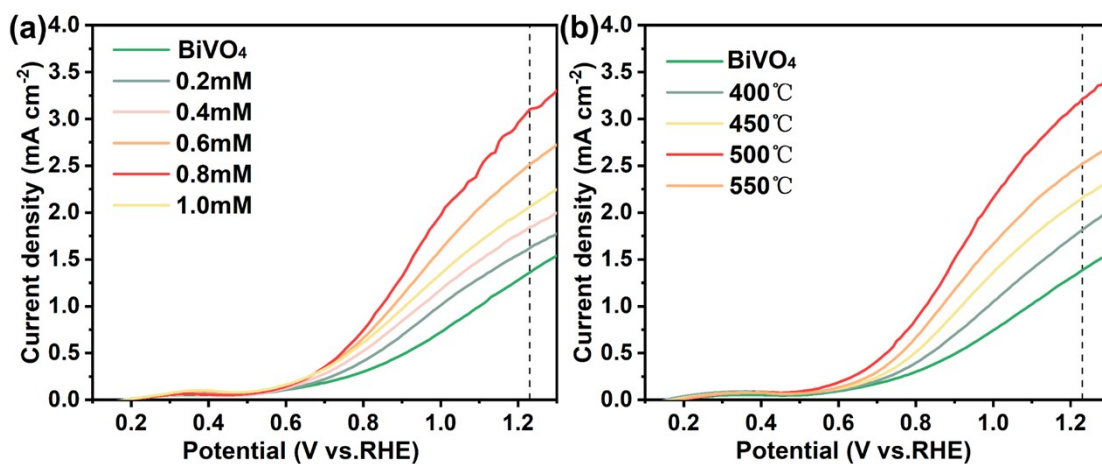


Fig. S1 LSV images optimized for (a) concentration and (b) temperature of S-BiVO<sub>4</sub>/WO<sub>3</sub>

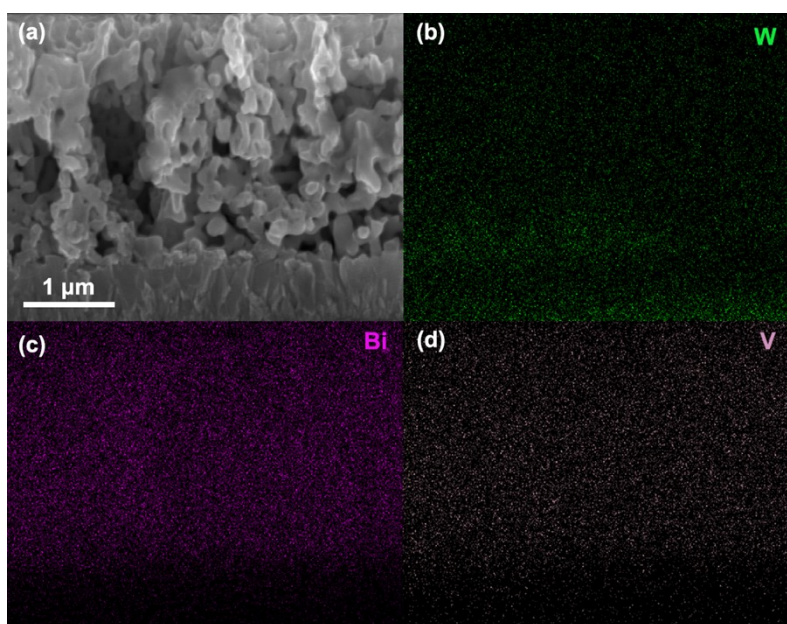


Fig. S2 The cross-section SEM image and corresponding element mapping images of S-BiVO<sub>4</sub>/WO<sub>3</sub>

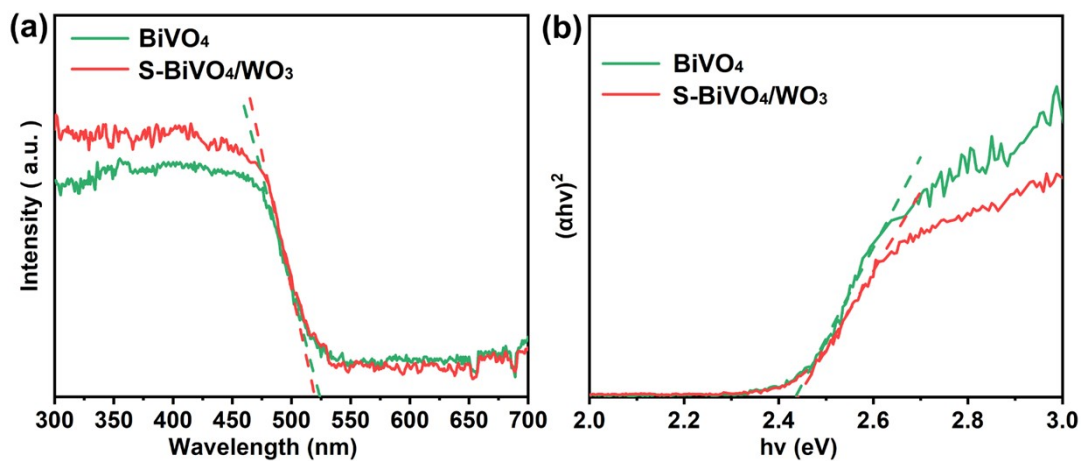


Fig. S3 UV-vis absorption images and (b) Tauc plots of BiVO<sub>4</sub> and S-BiVO<sub>4</sub>/WO<sub>3</sub>

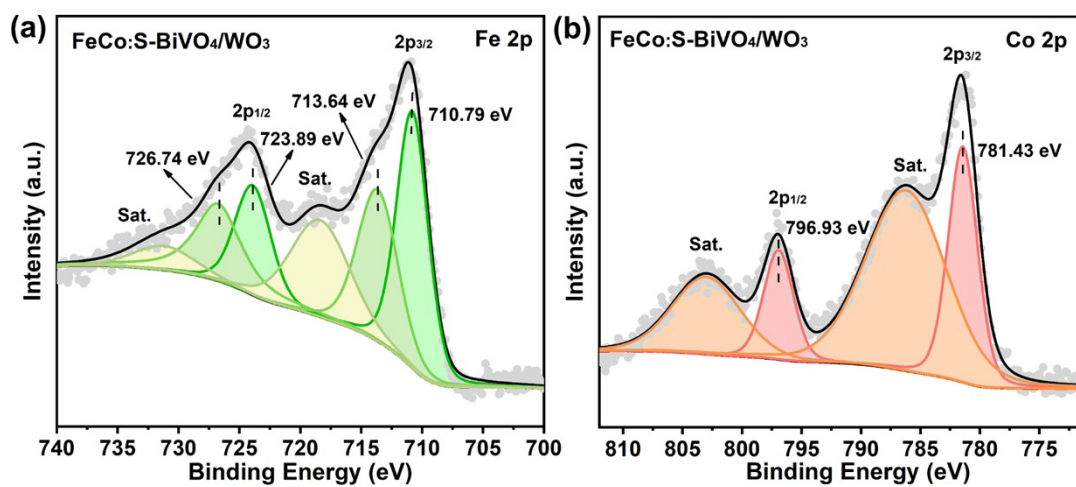


Fig. S4 XPS spectra of FeCo:S-BiVO<sub>4</sub>/WO<sub>3</sub>: (a) Fe 2p, (b) Co 2p

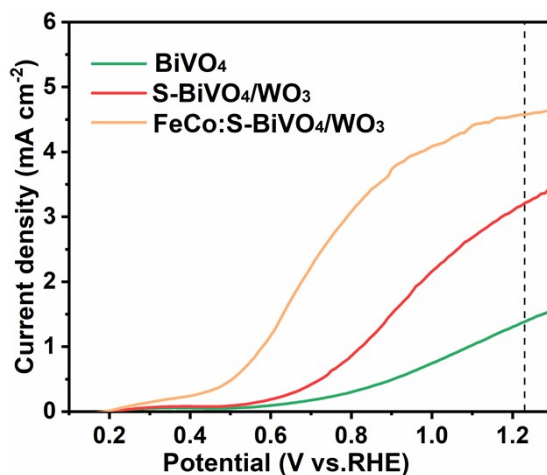


Fig. S5 LSV diagram of BiVO<sub>4</sub>, S-BiVO<sub>4</sub>/WO<sub>3</sub> and FeCo:S-BiVO<sub>4</sub>/WO<sub>3</sub>

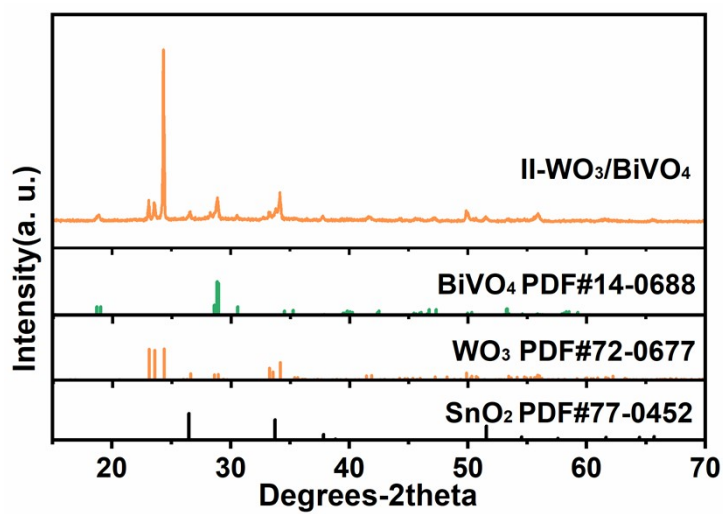


Fig. S6 XRD image of II-WO<sub>3</sub>/BiVO<sub>4</sub>

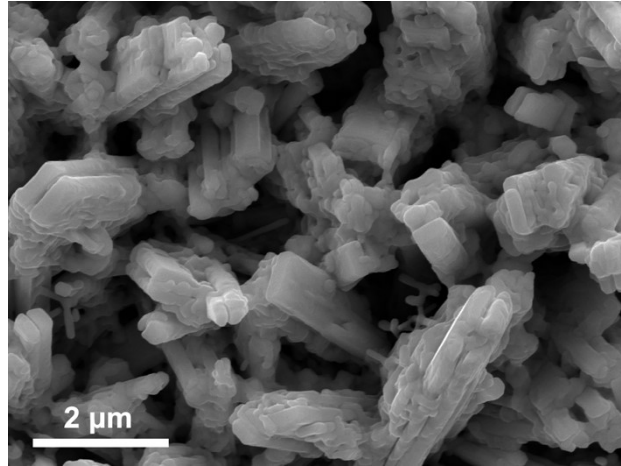


Fig. S7 SEM image of II-WO<sub>3</sub>/BiVO<sub>4</sub>

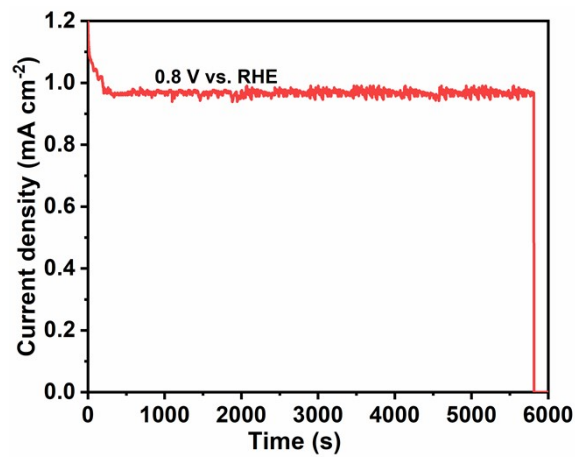


Fig. S8 *i*-*t* curves of S-BiVO<sub>4</sub>/WO<sub>3</sub>

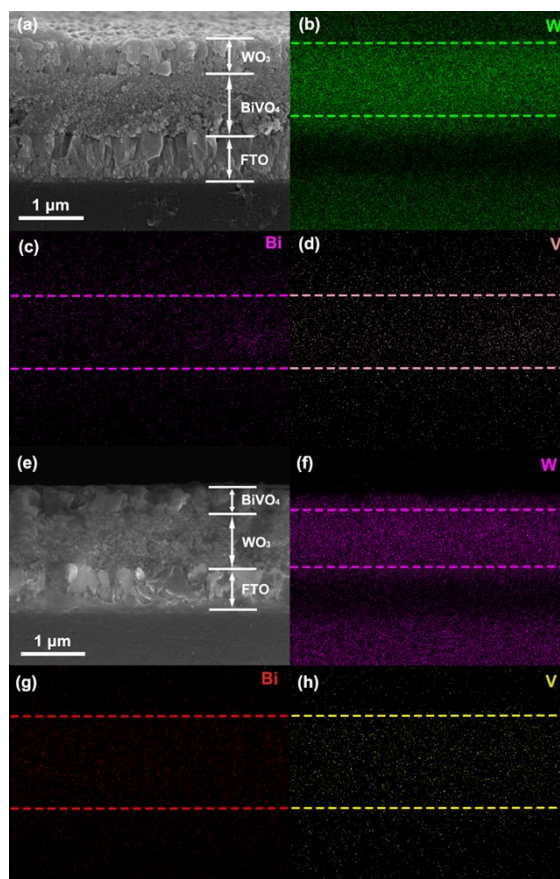


Fig. S9 The cross-section SEM and corresponding element mapping images of (a-d) S-BiVO<sub>4</sub>/WO<sub>3</sub> and (e-h) II- WO<sub>3</sub>/BiVO<sub>4</sub> prepared by the spin-coating method

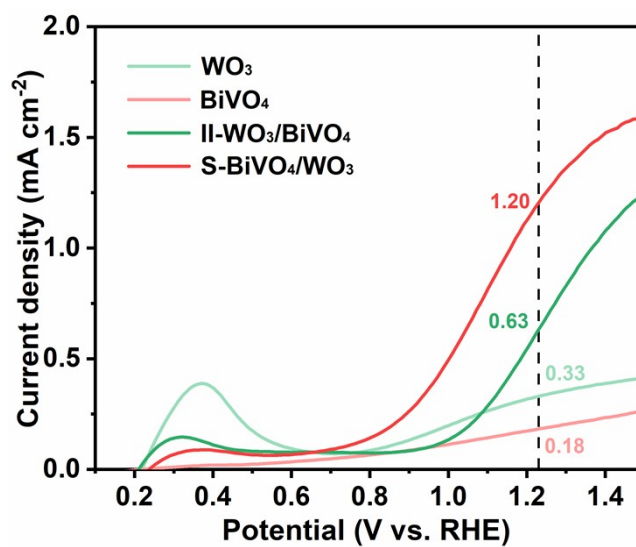


Fig. S10 LSV images of BiVO<sub>4</sub>, WO<sub>3</sub>, S-BiVO<sub>4</sub>/WO<sub>3</sub>, and II-BiVO<sub>4</sub>/WO<sub>3</sub> prepared by spin-coating method

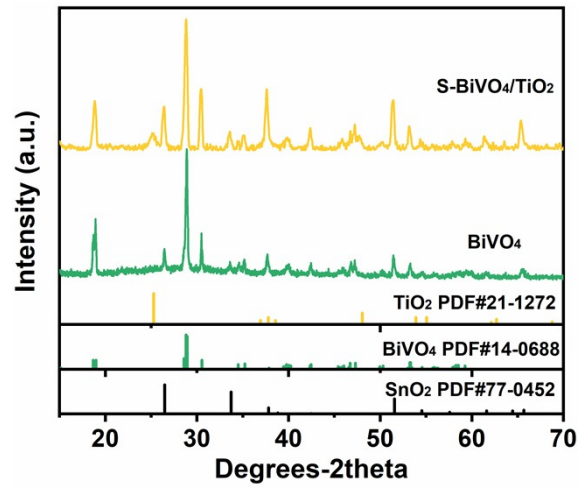


Fig. S11 XRD image of S-BiVO<sub>4</sub>/TiO<sub>2</sub>

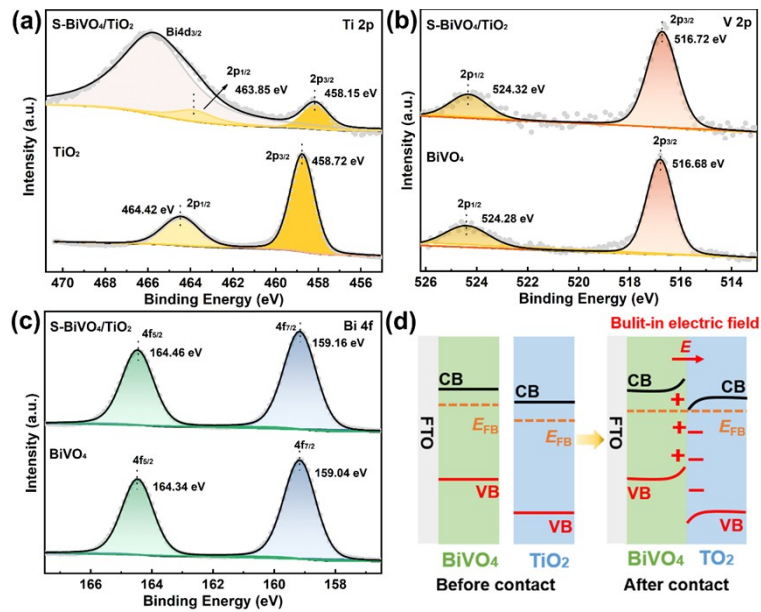


Fig. S12 XPS spectra of BiVO<sub>4</sub>, TiO<sub>2</sub> and S-BiVO<sub>4</sub>/TiO<sub>2</sub> composites: (a) Ti 2p, (b) V 2p, (c) Bi 4f,

(d) the schematic diagram of charge transfer of S-BiVO<sub>4</sub>/TiO<sub>2</sub> heterojunctions



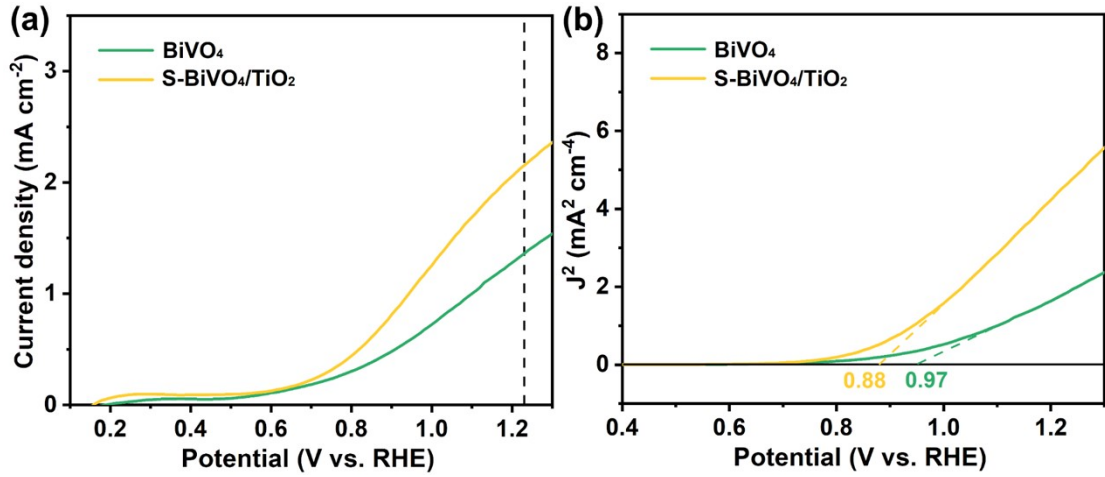


Fig. S13 (a) LSV diagram and (b)  $J^2$ - $V$  curves of  $\text{BiVO}_4$  and  $\text{S-BiVO}_4/\text{TiO}_2$

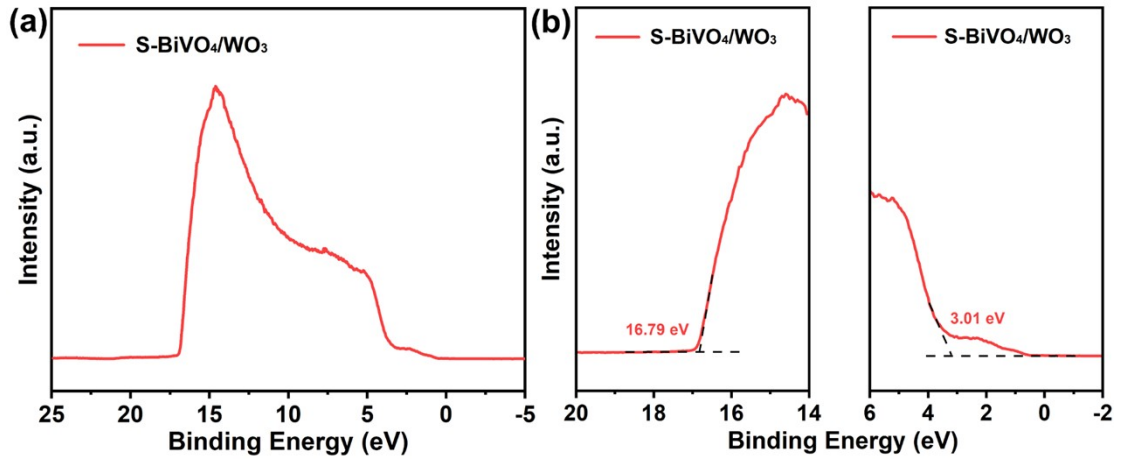


Fig. S14 (a) UPS spectrum and (b) the corresponding secondary electron cut-off edges and Fermi edges of  $\text{S-BiVO}_4/\text{WO}_3$

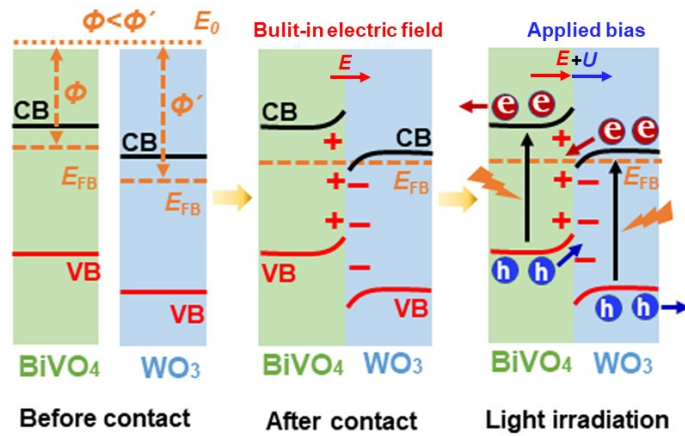


Fig. S15 The schematic diagram of charge transfer of  $\text{S-BiVO}_4/\text{WO}_3$  heterojunctions

## Reference

1. W. Ge, K. Liu, S. Deng, P. Yang and L. Shen, *Appl. Surf. Sci.*, 2023, **607**, 155036.
2. X. Zhao, J. Li, X. Song, X. Liu, W. Zhou, H. Wang and P. Huo, *Appl. Surf. Sci.*, 2022, **601**, 154246.
3. J. Su, L. Guo, N. Bao and C. A. Grimes, *Nano Lett.*, 2011, **11**, 1928-1933.
4. M. G. Lee, D. H. Kim, W. Sohn, C. W. Moon, H. Park, S. Lee and H. W. Jang, *Nano Energy*, 2016, **28**, 250-260.